# Obliquely projecting chiral alkyl chains and their precession around the long core axes in the smectic-*A* phase of an antiferroelectric liquid crystal

Bo Jin,[1] Zhihua Ling,[1] Yoichi Takanishi,[1] Ken Ishikawa,[1] Hideo Takezoe,[1] Atsuo Fukuda,[1] Masa-aki Kakimoto,[1] and Tomoya Kitazume[2]

[1]*Tokyo Institute of Technology, Department of Organic and Polymeric Materials, O-okayama, Meguro-ku, Tokyo 152, Japan*
[2]*Tokyo Institute of Technology, Department of Bioengineering, Nagatsuta, Midori-ku, Yokohama 226, Japan*

By deuterizing the chiral and achiral alkyl chains separately, we have observed the ir absorbance vs polarizer rotation angle for the $CH_2$ and phenyl ring stretching peaks in a prototype antiferroelectric liquid crystal, 4-(1-methylheptyloxycarbonyl) phenyl 4′-octyloxybiphenyl-4-carboxylate (MHPOBC). The angle between the chiral chain and core axes is more than 54.7° (the magic angle) even in the smectic-*A* (Sm-*A*) phase and the precession appears to be biased or hindered toward the tilt-plane normal in the chiral smectic-*C* (Sm-*C**) phase. [S1063-651X(96)00805-8]

PACS number(s): 61.30.Gd, 77.80.−e, 78.30.−j

Both in the chiral smectic-*C* (Sm-*C**) and smectic-$C_A$ (Sm-$C_A^*$) phases, the transverse permanent dipoles near the chiral center of the constituent molecules play an essential role in the emergence of ferroelectricity [1,2] and antiferroelectricity [3,4]; neither of them does emerge without these dipoles. However, the role in ferroelectricity differs from that in antiferroelectricity. The intermolecular interaction due to the Coulomb force among the permanent dipoles is not the direct cause of the ferroelectricity. The Sm-*C** low symmetry makes the transverse permanent dipoles align preferentially through the intermolecular interaction due to the attractive dispersion and repulsive steric forces; tilting together with molecular chilarity locally breaks the axial symmetry around the long molecular axes and induces in-layer spontaneous polarizations along the tilt-plane normal [2,5].

On the other hand, the Coulomb force among the permanent dipoles has been considered to directly cause the antiferroelectricity. Takanishi *et al.* [6] proposed the pairing model that the permanent dipoles form pairs in adjacent smectic layers. Quite recently, Miyachi *et al.* [7] suggested another possibility, the $P_X$ model, that the biased or hindered rotation of permanent dipoles about the long molecular axes tend to produce in-layer spontaneous polarizations parallel to the tilt plane, $P_X$'s, at the smectic layer boundaries; the existence of $P_X$'s themselves together with their interaction between the boundaries through the fluctuation force [8] results in the stabilization of the antiferroelectricity.

Neither of the models appears to be realistic, however, because antiferroelectric liquid crystals generally have the following two characteristic features: (1) the permanent transverse dipoles are not located at the end of the chiral alkyl chain [4,6], and (2) the smectic layer structure can approximately be depicted as an ordinary picture of molecules lying on equidistant planes [4,9]. If the chiral chain is bent extremely as actually observed in a crystal phase by Hori and Endo [10] or the molecules very much interdigitate with one another between adjacent layers, the Coulomb force among the permanent dipoles may become strong enough to stabilize the antiferroelectricity in liquid crystals. The purpose of this Rapid Communication is to show unambiguously that the chiral chain is, in fact, projecting obliquely from the core even in the smectic-*A* phase (Sm-*A*) and hence is considered precessing around the long core axis; the angle between the chiral chain and core axes is more than the magic angle, 54.7°. Such a bent molecular structure may allow the perma-
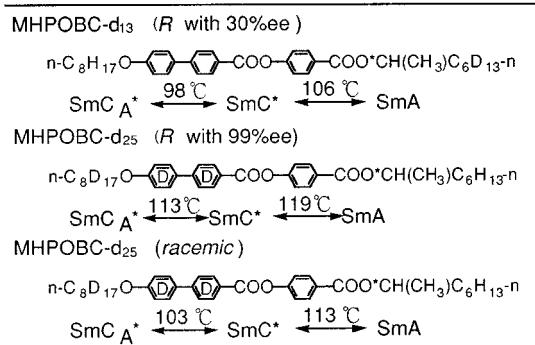
FIG. 1. The molecular formulas and phase sequences of samples used. The abbreviation ee means enantiomeric excess defined by ee=(R−S)/(R+S).
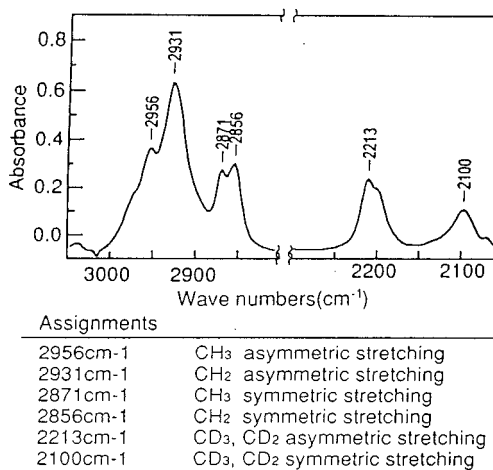


FIG. 2. Absorption spectra of $CH_2$, $CH_3$, $CD_2$, and $CD_3$ together with their peak wave numbers and assignments.
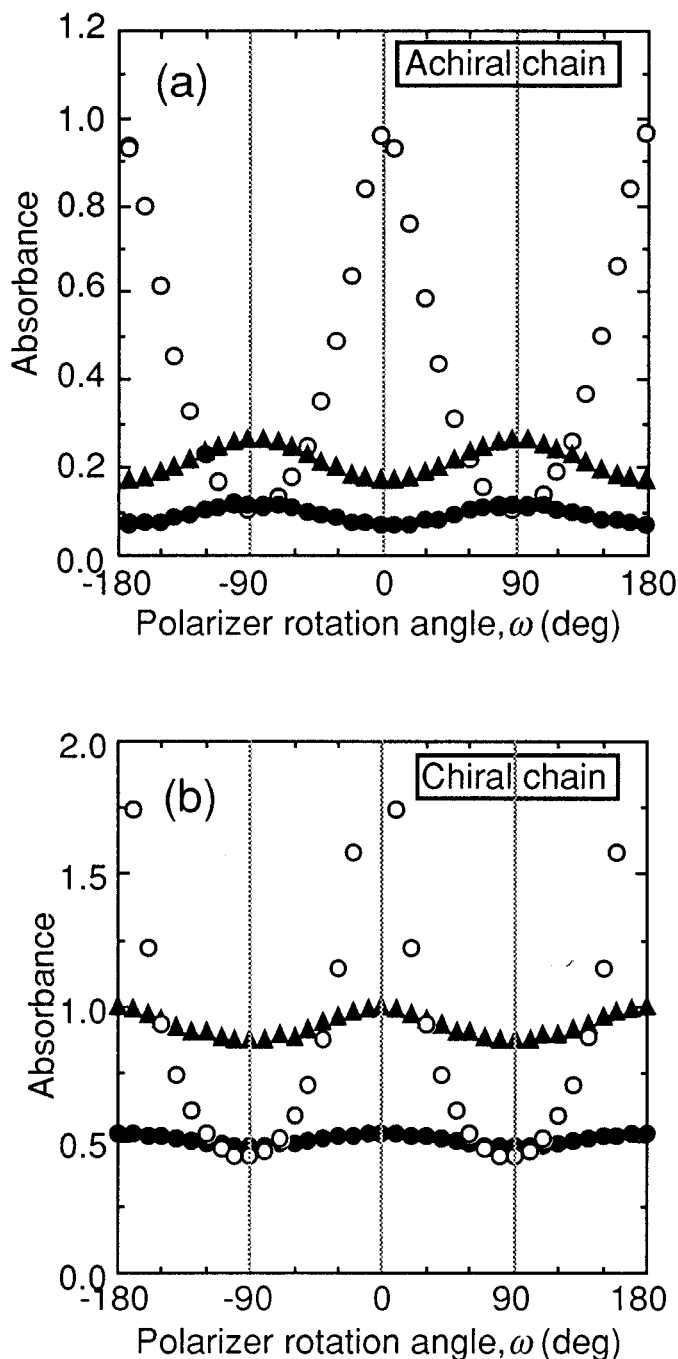
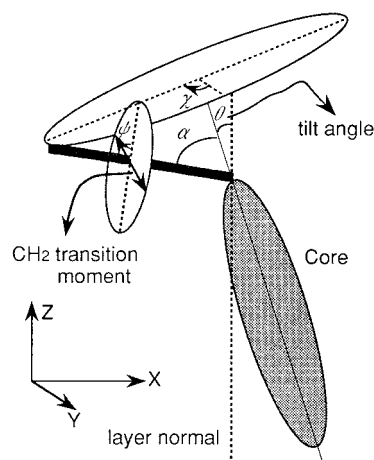| Assignments | |
|---|---|
| 2956cm-1 | CH₃ asymmetric stretching |
| 2931cm-1 | CH₂ asymmetric stretching |
| 2871cm-1 | CH₃ symmetric stretching |
| 2856cm-1 | CH₂ symmetric stretching |
| 2213cm-1 | CD₃, CD₂ asymmetric stretching |
| 2100cm-1 | CD₃, CD₂ symmetric stretching |

FIG. 4. A model of the transition dipole moment for the $CH_2$ stretching vibrations, situated on the alkyl chain and freely rotating about the chain axis. The chain itself makes the angle of $\alpha$ with the core axis and precesses around it.

and asymmetric stretching peaks, the separation between $CH_2$ and $CH_3$ is better than that of $CD_2$ and $CD_3$; consequently, we will mainly show the results obtained from the $CH_2$ peaks. However, the qualitatively similar results were also obtained from the $CD_2$ peaks. The phenyl ring stretching peak at 1604 $cm^{-1}$ was used to determine the average direction of the long molecular axis [7,11,12].

Figures 3(a) and 3(b) show the absorbance vs polarizer rotation angle observed in Sm-*A* of (*R*)-MHPOBC-$d_{13}$ and (racemic)-MHPOBC-$d_{25}$, respectively. Because of the partial deuterization indicated in Fig. 1, these figures give information about the achiral and chiral chains, separately. The angular dependence of the $CH_2$ stretching peaks, both asymmetric and symmetric, exhibits a conspicuous contrast between the achiral and chiral chains. In the achiral chain, it is out of phase with that of the phenyl ring stretching peak. In the chiral chain, on the other hand, it is in phase; moreover, the degree of polarization is very small. Five and seven $CH_2$ groups exist in the achiral and chiral chains, respectively, but their stretching vibrations show only two peaks, one asymmetric and the other symmetric; the alkyl chain conformation is changing temporally and spatially. We may be allowed to consider an average transition dipole moment
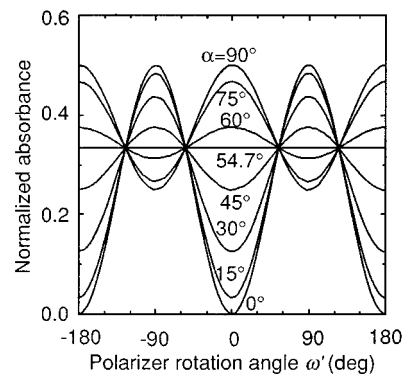


FIG. 3. Absorbance vs polarizer rotation angle in Sm-*A* measured at 130 °C using homogeneously aligned cell of (a) 4.0 $\mu$m thick (*R* with 30% ee)-MHPOBC-$d_{13}$ and (b) 9.6 $\mu$m thick (racemic)-MHPOBC-$d_{25}$. ○: Phenyl ring stretching; ▲: $CH_2$ asymmetric stretching; and ●: $CH_2$ symmetric stretching.

nent dipoles in adjacent layers to adequately interact through the Coulomb force.

Three partially deuterated samples were used, the molecular formulas and the phase sequences of which are summarized in Fig. 1. Homogeneously aligned cells were prepared and polarized infrared (ir) spectra were measured as described in previous papers [7,11]. Figure 2 illustrates absorption spectra of $CH_2$, $CH_3$, $CD_2$, and $CD_3$ together with their peak wave numbers and assignments. Both in the symmetric



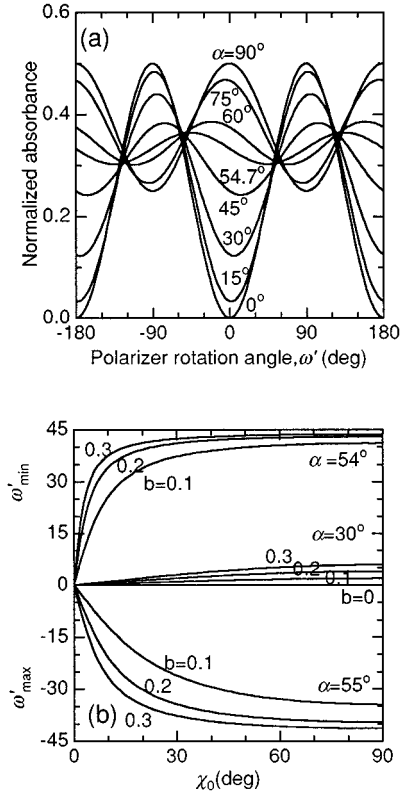FIG. 5. Normalized absorbance vs polarizer rotation angle in Sm-*A*, $A(\omega')$, calculated for various $\alpha$.

FIG. 6. (a) Normalized absorbance vs polarizer rotation angle in unwound Sm-$C^*$, $A(\omega')$, calculated for $b=0.3$, $\chi_0=60°$, and various $\alpha$. (b) Calculated $\omega'_{\min}(\chi_0,b;\alpha)$ for $\alpha=30°$ and $54°<54.7°$ and $\omega'_{\max}(\chi_0,b;\alpha)$ for $\alpha=55°>54.7°$. The degree of biasing, $b=0$, 0.1, 0.2, and 0.3 is used as a parameter.

of the $CH_2$ stretching vibrations, which is perpendicular to the average chain axis and is rotating freely around it.

Since the transition dipole moment of the phenyl ring stretching peak is parallel to the core axis, the out-of-phase relationship illustrated in Fig. 3(a) for the achiral chain is naturally expected if the chain axis is parallel to the core axis. The in-phase relationship illustrated in Fig. 3(b) for the chiral chain, on the other hand, requires a special explanation. Let us calculate the normalized absorbance by assuming the average transition dipole moment described above and by neglecting the sample anisotropy [7,11,12]. Several necessary angles are defined as depicted in Fig. 4; $\alpha$ is the angle between the chain and core axes, $\chi$ the azimuthal angle of the chain axis around the core axis, $\psi$ the rotation angle of the transition dipole moment around the chain axis, $\theta$ the tilt angle in Sm-$C^*$ which is zero in Sm-$A$, $\omega$ the polarizer rotation angle, and $\omega'=\omega-\theta$. The absorbance vs polarizer rotation angle is given by

$$A(\omega';\alpha)=\frac{1}{2\pi}\int_0^{2\pi}\int_0^{2\pi}f(\chi)(\sin\omega'\cos\chi\ \sin\psi$$

$$-\sin\omega'\cos\alpha\ \sin\psi-\cos\omega'\sin\alpha\ \cos\psi)^2 d\chi\ d\psi. \tag{1}$$



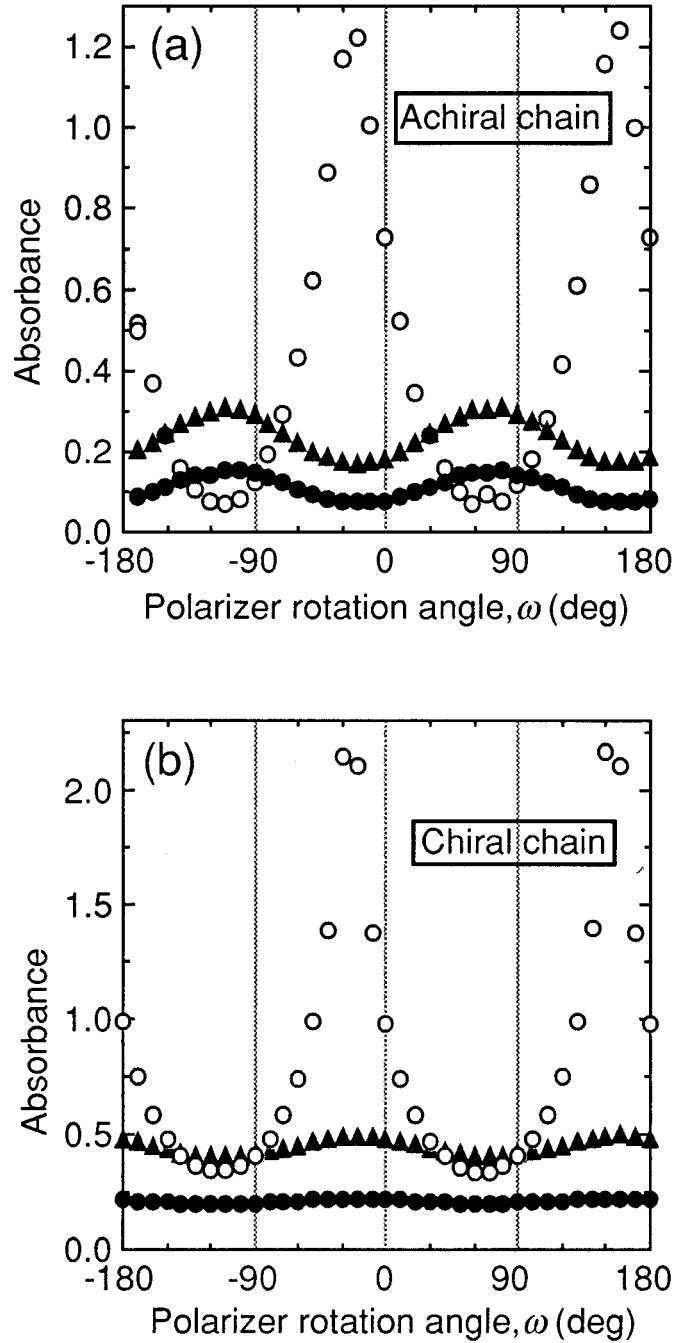FIG. 7. Absorbance vs polarizer rotation angle in electrically unwound Sm-$C^*$ homogeneously aligned cells, (a) for the achiral chain in 4.0 $\mu$m thick ($R$ with 30% ee)–MHPOBC-$d_{13}$ measured at 75 °C and 12.5 V $\mu$m$^{-1}$ and (b) for the chiral chain in 9.6 $\mu$m thick ($R$)-MHPOBC-$d_{25}$ measured at 100 °C and 9.5 V $\mu$m$^{-1}$. $\bigcirc$: Phenyl ring stretching; $\blacktriangle$: $CH_2$ asymmetric stretching; and $\bullet$: $CH_2$ symmetric stretching.

Here the distribution function in Sm-$A$ is $f(\chi)=1/(2\pi)$; the chain axis rotates freely around the core axis because of uniaxial Sm-$A$ symmetry.

Figure 5 shows the calculated normalized absorbance in Sm-$A$. At the magic angle, $\alpha=\cos^{-1}(1/\sqrt{3})=54.7°$, the absorbance does not depend on the polarizer rotation angle, $A(\omega;\alpha)=1/3$. The aforementioned in-phase and out-of-

phase relationships correspond to $\alpha > 54.7°$ and $\alpha < 54.7°$, respectively. In this way, Figure 3(b) unambiguously indicates that the chiral chain in Sm-*A* is obliquely projecting, precessing around the core axis; the angle between the chain and core axes is more than $54.7°$ but may probably be close to the magic angle because of the considerably small observed degree of polarization. Figure 3(a) also clearly shows that the achiral chain in Sm-*A* makes an angle $\alpha < 54.7°$ with the core axis. By taking account of the fact that not only the average transition moment but also the average chain axis itself is actually fluctuating, the rather large degree of polarization observed may indicate that the angle is far separated from the magic angle and rather close to zero.

The chiral chain precession will become biased or hindered in Sm-$C^*$ (Sm-*C*) and Sm-$C_A^*$ (Sm-$C_A$). By simply assuming a distribution function,

$$f(\chi) = \{1/(2\pi)\}\{1 + b\,\cos(\chi - \chi_0)\}, \qquad (2)$$

the absorbance vs polarizer rotation angle in electrically unwound Sm-$C^*$, $A(\omega';\alpha;b,\chi_0)$, is also given by Eq. (1). Here $\chi_0$ is the biased direction and $b$ the degree of biasing. Figure 6(a) illustrates some calculated results. $A(\omega';\alpha;b,\chi_0)$ is symmetric with respect to $\omega'_{min}$ or $\omega'_{max}$; depending on the sign of $\chi_0 > 0$ ($\chi_0 < 0$), $\omega'_{min}$ shifts from $0°$ toward $+45°$ ($-45°$) with an increase of $\alpha < 54.7°$, while $\omega'_{max}$ shifts from $0°$ toward $-45°$ ($+45°$) with a decrease of $\alpha > 54.7°$, respectively. The shift of $\omega'_{min}$ or $\omega'_{max}$ naturally depends on $b$ as illustrated in Fig. 6(b). Note that

$$\omega'_{min\ or\ max}(-\chi_0;b) = -\omega'_{min\ or\ max}(\chi_0;b).$$

Experimentally, we tried to observe the shift in unwound Sm-$C^*$ by applying an electric field; neither in the chiral chain nor in the achiral chain, however, could we so far confirm any clear shift, which appears to be smaller than $5°$ as shown in Fig. 7. This fact may indicate that the chiral chain precession is biased to the tilt plane normal ($\chi_0 \approx 0°$). It is also consistent with the above indication that $\alpha$ of the achiral chain is far separated from the magic angle and rather close to zero. Naturally, the shift is zero when $\chi_0 = 0$ or $\alpha = 0$. More detailed studies with improved accuracy, in particular, using not only homogeneous cells but also homeotropic ones, will surely give us reliable information about the alkyl chain directions in unwound Sm-$C_A^*$ as well as Sm-$C^*$. We are in the process of further investigations. Finally, it is-worthwhile noting that $^{13}$C NMR has clearly detected not only the chiral chain precession in Sm-*A* but also its hindrance or biasing in Sm-$C^*$ and Sm-$C_A^*$ [13].

*Note added in proof.* Ouchi *et al.* quite recently also concluded that the molecule has a bent structure even in Sm-*A* when they measured the smectic layer spacing of several homologous series in detail. [Y. Ouchi, Y. Yoshioka, H. Ishii, K. Seki, M. Kitamura, R. Noyori, Y. Takanishi, and I. Nishiyama, J. Mater. Chem. **5**, 2297 (1995)]

[1] R. B. Meyer, L. Liebert, L. Strzelecki, and P. Keller, J. Phys. (Paris) **36**, L69 (1975).

[2] R. B. Meyer, Mol. Cryst. Liq. Cryst. **40**, 33 (1977).

[3] A. D. L. Chandani, E. Gorecka, Y. Ouchi, H. Takezoe, and A. Fukuda, Jpn. J. Appl. Phys. **28**, L1265 (1989).

[4] A. Fukuda, Y. Takanishi, T. Isozaki, K. Ishikawa, and H. Takezoe, J. Mater. Chem. **4**, 997 (1994).

[5] T. Carlsson, B. Zeks, C. Filipic, and A. Levstik, Phys. Rev. A **42**, 877 (1990).

[6] Y. Takanishi, K. Hiraoka, V. K. Agrawal, H. Takezoe, A. Fukuda, and M. Matsushita, Jpn. J. Appl. Phys. **30**, 2023 (1991).

[7] K. Miyachi, J. Matsushima, Y. Takanishi, K. Ishikawa, H. Takezoe, and A. Fukuda, Phys. Rev. E **52**, R2153 (1995).

[8] R. Bruinsma and J. Prost, J. Phys. (France) II **4**, 1209 (1994).

[9] Y. Takanishi, A. Ikeda, H. Takezoe, and A. Fukuda, Phys. Rev. E **51**, 400 (1995).

[10] K. Hori and K. Endo, Bull. Chem. Soc. Jpn. **66**, 46 (1993).

[11] K. H. Kim, K. Ishikawa, H. Takezoe, and A. Fukuda, Phys. Rev. E **51**, 2166 (1995).

[12] W. G. Jang, C. S. Park, J. E. Maclennan, K. H. Kim, and N. A. Clark (unpublished).

[13] T. Nakai, Institute for Molecular Science (Okazaki, Japan), Report No. 7-802, 1996 (unpublished).